Bimetal based inorganic-carbonic anhydrase hybrid hydrogel membrane for CO_2 capture

Huan Wen[1], Lei Zhang[1], Yingjie Du[1], Ziyuan Wang[1], Yunhong Jiang[3], Hongjie Bian[2*], Jiandong Cui[1*], Shiru Jia[1]

[1]State Key Laboratory of Food Nutrition and Safety, Laboratory of Industrial Fermentation Microbiology, Ministry of Education, Tianjin University of Science and Technology, No 29, 13th, Avenue, Tianjin Economic and Technological Development Area (TEDA), Tianjin 300457, P R China

[2]Research Center for Fermentation Engineering of Hebei, College of Bioscience and Bioengineering, Hebei University of Science and Technology, 26 Yuxiang Street, Shijiazhang 050000, P R China

[3]HBBE, Department of Applied Science, Northumbria University, Newcastle, NE1 8ST, United Kingdom.

[*]Corresponding authors:

Hongjie Bian, E-mail: bianhongj@126.com

Jiandong Cui, E-mail: jdcui@tust.edu.cn, Tel: +86-022-60601598

Short title: Bimetal based hybrid hydrogel membrane for CO_2 capture

Abstract

In this study, we synthesized for the first time a bimetal-based inorganic-carbonic anhydrase (CA) hybrid nanoflower to immobilize CA using Cu^{2+} and Zn^{2+} instead of single metal ion. Subsequently, the synthesized bimetallic hybrid nanoflowers (CANF) were embedded into the poly(vinyl alcohol) (PVA)-chitosan (CS) hydrogel networks to obtain PVA/CS@CANF hydrogel membrane. The CANF exhibited a significantly higher activity recovery of 70% compared with 35% with CA/$Zn_3(PO_4)_2$ hybrid nanoflowers and 10% with CA/$Cu_3(PO_4)_2$ hybrid nanoflowers. The PVA/CS@CANF hydrogel membrane possessed excellent mechanical strength, high catalytic activity, and were easy to flow out without centrifugation or filtration. At the same time, the PVA/CS@CANF displayed higher thermostability, storage stability, and pH stability than free CA and CANF, and superior reusability and CO_2 capture capacity. The hydrogel membrane maintained more than 75% of its original activity after 8 cycles. However, CANF only maintained 12% of its original activity. Furthermore, the amount of $CaCO_3$ produced by PVA/CS@CANF membrane was 9.0-fold and 2.0-fold compared with free CA and CANF, respectively. Therefore, This approach to synthesizing bimetallic-based protein hybrid hydrogel membrane could have a bright future in CO_2 capture.

Keywords: Carbonic anhydrase; Bimetallic-based protein hybrid; Hydrogel membranes; Immobilization; CO_2 sequestration

1. Introduction

Nowadays, global warming remains a pressing issue globally [1]. It is well known that CO_2 emissions are responsible for the greenhouse effect [2,3]. To reduce the CO_2 emissions, CO_2 sequestration have attracted much attention. Various methods for capture and utilization of CO_2 have been proposed including the chemical adsorption, physical absorption, and enzymatic reactions [4-6]. In comparison, the use of enzymatic method has been paid more and more attention [7,8]. The carbonic anhydrase (CA) is a zinc-containing metalloenzyme that can accelerate the hydration of CO_2 [9–11]. However, low stability and poor reusability of free CA in the harsh conditions limits its industrial application [12,13]. Immobilization has been used to improve the stability and reusability of enzymes [14,15]. Decades ago, immobilized CA was successfully prepared using various materials including mesoporous silica [16], nanofibers [17], nanoparticles [18], and membranes [19]. The immobilized CA displayed better stability than free CA. However, the inactivation of enzyme is inevitable in the process of immobilization due to the change of enzyme structure, and the enhanced diffusion resistance between substrate and enzymes [20-22]. Recently, some novel methods for enzyme immobilization have been developed by co-precipitation of enzyme and inorganic components [23-26]. Especially, Ge et al developed an efficient method of enzyme immobilization, which called "enzymes-inorganic hybrid nanoflowers (HNF)"[27]. Compared with the immobilized enzymes with various supports, these HNF exhibited more effective in immobilization

due to high protein loading rate, mass-transfer limitation, and mild preparation conditions [27,28]. Lin et al. synthesized trypsin/$Cu_3(PO_4)_3$ HNF. The prepared hybrid nanoflowers showed 270% enhancement in enzymatic activity [29]. Similarly, Yin et al. used calcium chloride as the inorganic components to prepare α-chymotrypsin-inorganic HNF that exhibited 266% increase in catalytic activity compared with free α-chymotrypsin [30]. In addition, lipase-inorganic HNF exhibited 147% higher activity than free lipase[31]. Recently, CA-inorganic HNF were also synthesized, and displayed enhanced thermal stability and excellent capacity of CO_2 capture [13,32]. However, the soft nature of the HNF makes them serious disadvantages including low mechanical and reusability. Furthermore, the HNF can be easily degraded by acid, limiting its application range [33,34]. Therefore, there is an urgent need to find novel strategies to improve properties of the HNF. Generally, the HNF are formed by coordination interaction between enzymes and metal ions [27,35]. Metal ions play a role in morphology and activity of the HNF [32,37]. Until now, the previous reports focused on single metal ion-protein HNF. Limited information is available for multimetal based inorganic-proteins hybrid nanoflowers [28].

In this study, a novel bimetal-based inorganic-CA hybrid nanoflower (CANF) was developed to immobilize CA using bimetal ions (Cu^{2+} and Zn^{2+}) instead of individual metal ions, and then these CANF composites were embedded into the PVA/chitosan (CS) hydrogel membranes to obtain a novel immobilized CA for CO_2 capture

(PVA/CS@CANF) (Fig. 1). The synthesized CANF exhibited higher enzyme recovery activity than single metal-based Zn-CA hybrid nanoflowers and Cu-CA hybrid nanoflowers. The PVA/CS/CA@CANF membranes possessed excellent recyclability and stability characteristics including thermal stability, acid tolerance, and storage stability, and could be easily separated without centrifugation due to their superior mechanical strength. More important, these PVA/CS/CA@CANF displayed better CO_2 capture capability than free CA and CANF.

2. **Materials and Methods**

2.1 Materials

4-Nitrophenyl acetate (p-NPA) and CA (EC4.2.1.1) were purchased from Aladdin corporation (Shanghai, China). PVA with 1750±50 number-average degree of polymerization and CS with 80%-95% deacetylation were obtained from Tianjin Fuchen corporation (Tianjin, China).

2.2 Synthesis of bimetal CA hybrid nanoflower and PVA/CS@CANF membrane

The hybrid nanoflower was synthesized in a typical experiment with some modifications [38]. Firstly, 200 μl $CuSO_4$(120 mM) and 50 μl $ZnSO_4$ (120 mM) was mixed with 30 mL of a phosphate buffered saline (PBS) solution (10 mM, pH 7.4) containing 5 mg CA, and stored at 4 °C for three days. The produced precipitates were separated at 10,000 ×g, and washed by PBS. Finally, the precipitate was dried

by using lyophilizer. For PVA/CS@CANF enzyme membrane, PVA (6 wt%), CS (1 wt%) and CANF (5 mg) were mixed, and repeatedly frozen in -20 °C for 12 h and thawed for 30 min at room temperature.

2.3 Activity assay

The activities of free CA and immobilized CA were measured by hydrolysis of p-NPA to p-NP based on the method described prescribed [39-42]. Briefly, CA samples were mixed with PBS (10 mM, pH 7.4) containing p-NPA (3 mM). After reaction 3 min at 25 °C, the supernatant was determined at 348 nm by UV-visible spectrophotometer (UV752, Sahnghai Optical Instrument, China). One unit of CA activity refers to the amount of CA used to hydrolyze 1 μmol 4-NPA per minute. The activity recovery of immobilized enzyme was calculated as given in Eq.

$$\text{Activity recovery}(\%) = \frac{\text{Total of immobilized CA activity}}{\text{Free CA activity}} \times 100\%$$

2.4 Characterization of CANF and PVA/CS@CANF

Scanning electron microscope (SEM, Hitachi S4800) was used to observe the morphologies of CANF and PVA/CS@CANF. Fourier transform infrared (FT-IR) spectra was conducted in the region 400-4000 cm^{-1} using by FT-IR spectroscopy (FTIR, NEXUS870). The elemental analysis of the immobilized CA was obtained by using energy-dispersive spectrometer (EDS). The CA molecules were labeled by FITC and characterized by confocal laser scanning microscope (CLSM, Leica Camera

AG). An electronic universal testing machine (CMT4503, China) was used to determine mechanical properties of the PVA/CS@CANF membrane.

2.5 Stability measurements

Storage stability of CA samples was measured by storing them in PBS (10 mM, pH 7.4) at 25 °C, and their residual activities were determined every three days. For the determination of thermal stability, CA samples were treated at 65 °C for 5-25 min. pH stability was measured after incubation of CA samples for 30 min in the different pH buffers (5.5-10.5). The reusability of the CANF and PVA/CS@CANF in continuous operation was evaluated for the hydrolysis of p-NPA during 8 reuse cycles. After one cycle, the CANF and PVA/CS@CANF was collected from the media, and washed three times with deionized water, and then carried out next round of reaction.

2.6 CO_2 conversion

The CO_2 conversion experiment was carried out according to the approach described by previous reports [13,43-45]. Briefly, 25 mL of buffer solution (50 mM PBS, pH 7.0) was bubbled with CO_2 gas for 30 min, and 50 mg of immobilized enzyme (the same enzyme activity as free CA) was added to start the reaction at room temperature for 30 min. Subsequently, the immobilized CA was separated from the mixture solution, and washed with with buffer solution, and used to convert CO_2 again. After 8 cycles, the supernatant was gathered and mixed with $CaCl_2$ solution (10%) to form

carbonate precipitation. The precipitates were filtered by 0.2 μm membrane filters (Millipore) and dried.

3. Results and discussion

3.1 Synthesis and characterization of PVA/CS@CANF

The illustration for synthesis of the PVA/CS@CANF was shown in Fig. 1. The CANF was synthesized in PBS (10 mM, pH 7.4) solution containing CA, $CuSO_4$ and $ZnSO_4$ for 72 h at 4 °C. Subsequently, the CANF was encapsulated in the PVA/CS hydrogel network to form PVA/CS@CANF membrane. SEM showed that the CANF exhibited a porous spherical-like structures (Fig. 2a), whereas CA/$Cu_3(PO_4)_2$ hybrid and CA/$Zn_3(PO_4)_2$ HNFs displayed flower-like morphology with compact structure and large particles with amorphous shape, respectively (Fig. 2b and Fig. 2c). In addition, the PVA/CS hydrogel possessed smooth surface with micron pores (Fig. 2d). The porous structure is favorable for the diffusion of substrates and products, and it is advantageous for the improvement of catalytic activity. In contrast, PVA/CS@CANF hydrogel membrane exhibited rough surface with porous structure (Fig. 2e). The CANF particles could be clearly observed in the internal space of PVA/CS@CANF hydrogel membrane (Fig. 2f), suggesting that the CANF was embedded into the PVA/CS@CANF hydrogel membrane. The FTIR spectra displayed the peaks at 1650 cm^{-1} of protein and at 1050 cm^{-1} of P-O in the PVA/CS@CANF, suggesting the existence of CA and phosphate groups in the PVA/CS hydrogel membrane (Fig. 3)

[46]. Furthermore, the typical absorption peaks at 3300 cm^{-1} and at 2930 cm^{-1} were contributed to the vibrations of the -OH, -CH and -CH_2−OH groups of PVA and CS, respectively [47,48]. Meanwhile, CLSM images had abundant green fluorescence in the CANF and the PVA/CS@CANF hydrogel membrane (Fig. 4), suggesting the existence of CANF in the hydrogel membrane. Besides, Cu element and Zn element in the PVA/CS@CANF hydrogel membrane were observed, which could derived from $Cu_3(PO_4)_2$ and $Zn_3(PO_4)_2$, further indicating the presence of CANF (Fig. 5). These results further confirmed that the CANF was successfully embedded into the PVA/CS@CANF hydrogel membrane. Generally, the immobilized enzymes should have a certain mechanical strength to resist the external shear forces of handling during centrifugation and filtration [12,49]. Likewise, the hybrid nanoflowers with low mechanical strength usually exhibit low operation stability [50,51]. As rigid polymeric matrix, PVA/CS hydrogel membrane was used as superior immobilized carrier [12,52,53]. Here, we measured the mechanical properties of the PVA/CS/CA@CANF. The hydrogel membrane exhibited high compressive resistance and superior tensile properties. The tensile strength and Tensile stain at break were 0.984 ± 0.036 MPa and 6.675% ± 0.399%, respectively (Table 1). The superior mechanical properties of the PVA/CS/CA@CANF would help to improve the long-term operational stability of CANF.

3.2 The activity of CANF and PVA/CS@CANF

As known, activity recovery is an important parameter for the immobilized enzymes. Therefore, the CA/$Cu_3(PO_4)_2$, CA/$Zn_3(PO_4)_2$ CA and CANF was synthesized at the same conditions via self-assembly in the presence of Cu^{2+}, Zn^{2+} and Cu^{2+}/Zn^{2+}, respectively. The maximum activity recovery of the CA/$Cu_3(PO_4)_2$, CA/$Zn_3(PO_4)_2$ CA and CANF was compared. The results were shown in Fig. 6a. It was found that the novel multimetal-based CANF exhibited significant enhancement in activity recovery compared with the CA/$Cu_3(PO_4)_2$ and CA/$Zn_3(PO_4)_2$. The maximum activity recovery of the CANF was 70%, whereas CA/$Cu_3(PO_4)_2$ and CA/$Zn_3(PO_4)_2$ was only 10% and 35%, respectively. The maximum activity recovery of the CANF was 7-folds and 2-folds higher than CA/$Cu_3(PO_4)_2$ and CA/$Zn_3(PO_4)_2$. In addition, effects of the mole ratio of Cu ion and Zn ion on the activity recovery of CANF were investigated. It was found that the activity recovery of CANF was the higher when the mole ratio of Cu ion and Zn ion was 4:1 (data not shown). These results indicated that the Cu/Zn bimetal based CA hybrid nanoflowers are more effective than the individual metal CA hybrid nanoflowers. The previous reports showed that different binding sites of metal ions on enzyme proteins could lead to different properties of the hybrid nanoflowers [54,55]. Here, the enhancement activity recovery of the CANF could be due to synergistic influence of Cu^{2+} and Zn^{2+} on different binding sites of CA. Besides, effects of mass ratio of PVA and CS on activity recovery of the PVA/CS@CANF were investigated at the same weight of CANF (5 mg). Activity recovery increased with decrease of PVA quantity. The maximum activity recovery of the

PVA/CS@CANF was obtained when mass ratio of PVA and CS was 4 (Fig. 6b). Meanwhile, influences of temperature and pH on the enzymatic activity of all CA samples were investigated. The optimal temperature of free CA and CANF was presented at 56 °C, whereas the PVA/CS@CANF was at 60 °C (Fig. 6c). Furthermore, the CANF and PVA/CS@CANF exhibited more than 80% relative activities at high temperature (58-62 °C). In contrast, free CA displayed low activity. Especially, the PVA/CS@CANF still retained more than 90% relative activity at higher temperature (58-62 °C). These results showed that the PVA/CS@CANF could possess better thermal stability than free CA and CANF. In addition, the optimal pH of free CA and CANF was showed at 8.0. However, the PVA/CS@CANF exhibited highest activity at pH 8.5(Fig. 6d).

3.3 Stability of free CA and immobilized CA

To further investigate the effects of temperature on stability of free CA and immobilized CA, CA samples were incubated at 65 °C for a certain time. The thermal stability curves of the CANF, PVA/CS@CANF and free CA were shown in Fig. 7a. As could be seen the free CA, CANF, and PVA/CS@CANF exhibited differently when exposed to the heat. Free CA maintained only 20% of initial activity after treatment for 5 min. However, the CANF and PVA/CS@CANF still maintained more than 80% of their initial activity. Furthermore, it was noted that the PVA/CS@CANF exhibited higher thermal stability than the CANF during the whole treating time. A similar result was obtained while evaluating pH stability of free CA and immobilized

CA (Fig. 7b). The PVA/CS@CANF was more stable than the free CA and CANF within the tested pH range (pH 5.5-10.5). The PVA/CS@CANF retained 65% of its initial activity after treatment 30 min at pH 5.5. However, free CA and CANF only maintained less than 40% of their initial activity. The enhanced pH and thermal stability of the PVA/CS@CANF could due to the fact that PVA/CS hydrogel membrane may produce a suitable microenvironment to decrease the change of CA conformation at harsh environment. The PVA/CS hydrogel membrane plays a "protection shell" to avoid heat and chemical damage to enzymes [54,55]. In addition, The CANF and PVA/CS@CANF showed higher storage stability than free CA (Fig. 7c). Free CA maintained only 65% of its original activity after 12 days. However, the PVA/CS@CANF retained 100% of it initial activity. Furthermore, free CA lost 78% of its original activity after 18 days, whereas the CANF and PVA/CS@CANF remained 88% and 56% of their original activity, respectively. The enhancement storage stability could be due to the combination of confinement effect with the encapsulation of enzyme in the PVA/CS hydrogel membrane. Besides, one of the main objective of this work is to overcome low mechanical and reusability of hybrid nanoflowers. Here, the reusability of immobilized CA were estimated. The results were shown in Fig. 7d. The CANF maitianed only 13% of its original activity after 8 cycles. However, for the PVA/CS@CANF, above 75% of its original activity was still remained. The previous reports showed that the hybrid nanoflowers exhibited a remarkable decrease in the activity in the process of continuous reuses due to the loss

and destruction of the enzyme immobilized as hybrid nanoflowers during the centrifugation and washing [34,56]. In comparison, the PVA/CS/CA@CANF in this study could be recovered directly using a pair of tweezers without high speed centrifugation, avoiding the damage of the CANF caused by high shear force. This result suggested that the hydrogel membrane accelerated recovery of CANF, improving reusability.

3.4 Conversion of CO_2 to $CaCO_3$

The ability of the CANF and PVA/CS@CANF to catalyze CO_2 hydration was evaluated by carbonization experiments, and the results were shown in Figure 8. The total production of $CaCO_3$ in the system of free enzyme, CANF and PVA/CS@CANF was 14.76 mg, 76.27 mg and 135.22 mg under experimental conditions in this study, respectively. $CaCO_3$ yield obtained using CANF and PVA/CS@CANF was 5.2 and 9.2 fold higher than free CA, respectively. This result showed that PVA/CS@CANF membrane possessed better CO_2 sequestration capacity compared with free CA and CANF. It may be due to the following reasons: 1. the low mechanical strength of CANF makes them difficult to be recovered and reused; 2. the pH value of the solution is acidic with the hydration of CO_2 that destroy the structure of CANF. However, the PVA/CS@CANF membrane with excellent mechanical strength could maintain enzyme activity due to their convenient recovery and the protection effects of PVA/CS membrane for the CANF. Furthermore, SEM images exhibited that

produced $CaCO_3$ by free CA and immobilized CA was calcite particles (a stable state of $CaCO_3$), suggesting the hydration of CO_2 to bicarbonate.

4. Conclusion

In conclusion, a bimetal-based inorganic-CA hybrid nanoflower was developed to immobilize CA using Cu^{2+} and Zn^{2+}. Compared with individual metal ion CA/$Zn_3(PO_4)_2$ and CA/$Cu_3(PO_4)_2$ hybrid nanoflowers, the bimetal based inorganic-CA hybrid exhibited 2-fold and 7-fold higher activity recovery. Furthermore, CANF was successfully encapsulated into the PVA/CS hydrogel membrane to form \PVA/CS@CANF membrane with excellent mechanical strength. The PVA/CS@CANF exhibited higher thermal stability, pH stability, and storage stability than free CA and CANF due to protection effects of PVA/CS membrane. Furthermore, the PVA/CS@CANF membrane with excellent mechanical strength can be easily separated from reaction solution to reuse without high speed centrifugation, improving reusability. Particularly, the PVA/CS@CANF could efficiently capture CO_2. The quantity of $CaCO_3$ produced by PVA/CS@CANF was 9.0- and 2.0-fold higher than free CA and CANF, respectively. Therefore, this approach to synthesizing bimetallic-based protein hybrid hydrogel membranes could have significant application prospects in CO_2 capture.

Acknowledgements

This work is partially supported by the Open Project Program of State Key Laboratory of Food Nutrition and Safety, Tianjin University of Science & Technology (project no. SKLFNS-KF201904). Dr. J. D. Cui also thanks supports from the Key Projects of Tianjin Natural Science Foundation, China (project no. 19JCZDJC38100), and the Foundation (No. 19272809D) of Key R & D projects of science and Technology Department of Hebei Province.

References

[1] M. Hussain, A.R. Butt, F. Uzma, R. Ahmed, T. Islam, B. Yousaf, A comprehensive review of sectorial contribution towards greenhouse gas emissions and progress in carbon capture and storage in Pakistan, Greenh. Gases Sci. Technol. 9 (2019) 617–636.

[2] J.D. Shakun, P.U. Clark, F. He, S.A. Marcott, A.C. Mix, Z. Liu, B. Otto-Bliesner, A. Schmittner, E. Bard, Global warming preceded by increasing carbon dioxide concentrations during the last deglaciation, Nature. 484 (2012) 49–54.

[3] R. Monastersky, Global carbon dioxide levels near worrisome milestone, Nature. 497 (2013) 13–14.

[4] C. Yamali, H. I. Gul, C. Kazaz, S. Levent, I. Gulçin, Synthesis, structure elucidation, and in vitro pharmacological evaluation of novel polyfluoro substituted pyrazoline type sulfonamides as multi-target agents for inhibition of acetylcholinesterase and carbonic anhydrase I and II enzymes, Bioorg Chem. 2020, 96, 103627.

[5] S. Bal, R. Kaya, Y. Gök, P. Taslimi, A. Aktaş, M. Karaman, I. Gulcin, Novel 2-methylimidazolium salts: synthesis, characterization, molecular docking, and carbonic anhydrase and acetylcholinesterase ınhibitory properties. Bioorg Chem, 2020, 94, 103468.

[6] A. Biçer, R. Kaya, G. Yakali, M. S. Gultekin, G. T. Cin, I. Gulcin, Synthesis of

novel β-amino carbonyl derivatives and their inhibition effects on some metabolic enzymes. J. Mol Struct, 2020, 1204, 127453.

[7] D. J. Farrelly, C. D. Everard, C. C. Fagan, K. P. McDonnell, Carbon sequestration and the role of biological carbon mitigation: A review. Renewable Sustainable Energy Rev. 2013, 21, 712−727.

[8] J. F. Shi, Y. J. Jiang, Z. Y. Jiang, X. Y. Wang, X. L. Wang, S. H. Zhang, P. P. Han, C. Yang, Enzymatic conversion of carbon dioxide. Chem. Soc. Rev. 2015, 44, 5981−6000.

[9] M. Vinoba, M. Bhagiyalakshmi, S.K. Jeong, Y. Yoon, S.C. Nam, Capture and sequestration of CO2 by human carbonic anhydrase covalently immobilized onto amine-functionalized SBA-15, J. Phys. Chem. C 115 (2011) 20209-20216.

[10] B.K. Shanbhag, B.Y. Liu, J. Fu, V.S. Haritos, L.Z. He, Self-assembled enzyme nanoparticles for carbon dioxide capture, Nano Lett. 16 (2016) 3379-3384.

[11] I. Iliuta, M. Iliuta, Investigation of CO_2 removal by immobilized carbonic anhydrase enzyme in a hollow-fiber membrane bioreactor, AICHE J. 63 (2017) 2996-3007.

[12] M. Vinoba, D.H. Kim, K.S. Lim, S.K. Jeong, S.W. Lee, M. Alagar, Biomimetic sequestration of CO_2 and reformation to CaCO3 using bovine carbonic anhydrase immobilized on SBA-15, Energy Fuel 25 (2011) 438-445.

[13] S. Z. Ren, Y. X. Feng, H. Wen, C. H. Li, B. T. Sun, J. D. Cui, S. R. Jia,

Immobilized carbonic anhydrase on mesoporous cruciate flower-like metal organic framework for promoting CO_2 sequestration, Inter. J. Biol. Macromol, 117 (2018) 189-198.

[14] D.A. Cowan, R. Fernandez-Lafuente, Enhancing the functional properties of thermophilic enzymes by chemical modification and immobilization, Enzym. Microb. Technol. 49 (2011) 326-346.

[15] R. Fernandez-Lafuente, Stabilization of multimeric enzymes: strategies subunit dissociation, Enzym. Microb. Technol. 45 (2009) 405-418.

[16] H. S. Kim, S. G. Hong, K. M. Woo, V. T. Seijas, S. Kim, J. W. Lee, J. B. Kim, Precipitation-based nanoscale enzyme reactor with improved loading, stability, and mass transfer for enzymatic CO_2 conversion and utilization, ACS Catal. 8(2018) 6526 −6536.

[17] S. S. W. Effendi, C. Y. Chiu, Y. K. Chang, I. S. Ng, Crosslinked on novel nanofibers with thermophilic carbonic anhydrase for carbon dioxide sequestration, Inter. J. Biol. Macromol, 2019, doi: 10.1016/j.ijbiomac.2019.11.234.

[18] H. K. Kim, D. R. Kim, I. T. Hwang, Sequestration of CO_2 into $CaCO_3$ using carbonic anhydrase immobilization on functionalized aluminum oxide, 55(2019) 375-379.

[19] A. Bednár, N. Nemestóthy, P. Bakonyi, L. Fülöp, G. Zhen, X. Lu, T. Kobayashi, G. Kumar, K. Xu, K. Beĺafi-Bakó, Enzymatically-boosted ionic liquid

gas separation membranes using carbonic anhydrase of biomass origin. Chem. Eng. J. 303(2016) 621-626.

[20] S.W. Ding, A.A. Cargill, I.L. Medintz, J.C. Claussen, Increasing the activity of immobilized enzymes with nanoparticle conjugation, Curr Opin Biotech. 34 (2015) 242-250.

[21] J. Ge, D.N. Lu, Z.X. Liu, Z. Liu, Recent advances in nanostructured biocatalysts, Biochem Eng J. 44 (2009) 53-59.

[22] H.R. Lee, M. Chung, M.I. Kim, S.H. Ha, Preparation of glutaraldehyde-treated lipase-inorganic hybrid nanoflowers and their catalytic performance as immobilized enzymes, Enzyme. Microb. Tech. 105 (2017) 24-29.

[23] C. Hu, Y. Bai, M. Hou, Y. Wang, L. Wang, X. Cao, C.-W. Chan, H. Sun, W. Li, J. Ge, K. Ren, Defect-induced activity enhancement of enzyme-encapsulated metal-organic frameworks revealed in microfluidic gradient mixing synthesis, Sci. Adv. 6(2020)eaax5785.

[24] X. Wu, H. Yue, Y. Zhang, X. Gao, X. Li, L. Wang, Y. Cao, M. Hou, H. An, H. Gu, L. Zhang, S. Li, W. Lou, J. Ma, H. Lin, Y. Fu, W. Wei, R. N. Zare, J. Ge, Packaging and delivering enzymes by amorphous metal-organic frameworks. Nat. Commun, 10(2019)5165.

[25] Y. Cao, X. Li, J. Xiong, L. Wang, L. Yan, J. Ge, Investigating the origin of high efficiency in confined multienzyme catalysis Nanoscale. 11(2019) 22108-22117.

[26] X. Wu, J. Ge, C. Yang, M. Hou, Z. Liu, Facile synthesis of multiple enzyme-containing metal-organic frameworks in a biomolecule-friendly environment. Chem Commun. 51(2015)13408-13411.

[27] J. Ge, J. Lei, R.N. Zare, Protein–inorganic hybrid nanoflowers, Nat. Nanotechnol. 7 (2012) 428-432.

[28] S. K.S. Patel, H. Choi, J. K. Lee, Multimetal-based inorganic-protein hybrid system for enzyme immobilization, ACS Sustainable Chem. Eng. 7(2019) 13633−13638.

[29] Z. Lin, Y. Xiao, L. Wang, Y. Yin, J. Zheng, H. Yang, G. Chen, Facile synthesis of enzyme-inorganic hybrid nanoflowers and their application as an immobilized trypsin reactor for highly efficient protein digestion. RSC.Adv. 4 (2014) 13888-13891.

[30] Y. Yin, Y. Xiao, G. Lin, Q. Xiao, Z. Lin, Z. Cai, An enzyme-inorganic hybrid nanoflower based immobilized enzyme reactor with enhanced enzymatic activity, J. Mater. Chem. B. 3 (2015) 2295-2300.

[31] B. Zhang, P. Li, H. Zhang, H. Wang, X. Li, L. Tian, N. Ali, Z. Ali, Q. Zhang, Preparation of lipase/$Zn_3(PO_4)_2$ hybrid nanoflower and its catalytic performance as an immobilized enzyme, Chem. Eng. J. 291 (2016) 287-297.

[32] L. L. Dan, H. Li, Y. T. Zhang, Synthesis of hybrid nanoflower-based carbonic anhydrase for enhanced biocatalytic activity and stability, ACS Omega, 3(2018) 18234-18241.

[33] Z. X. Lei, C. L. Gao, Y. T. He, W. D. Ma, Z. Lin, Recent advances in biomolecule immobilization based on self-assembly: organic–inorganic hybrid nanoflowers and metal–organic frameworks as novel substrates, J. Mater. Chem. B, 6(2018) 1581-1594.

[34] M. F. Li, M. Y. Luo, F. Li, W. W. Wang, K. Liu, Q. Z. Liu, Y. D. Wang, Z. T. Lu, D. Wang, Biomimetic copper-based inorganic–protein nanoflower assembly constructed on the nanoscale fibrous membrane with enhanced stability and durability, J. Phys. Chem. C, 120(2016)17348-17356.

[35] J. D. Cui, S. R. Jia, Organic-inorganic hybrid nanoflowers: A novel host platform for immobilizing biomolecules, Coordin Chem. Rev, 352 (2017) 249-263.

[36] S. Escobar, S. Velasco-Lozano, C.H. Lu, Y.F. Lin, M. Mesa, C. Bernal, F. López-Galleqo, Understanding the functional properties of bio-inorganic nanoflowers as biocatalysts by deciphering the metal-binding sites of enzymes, J. Mater. Chem. B. 5 (2017) 4478–4486.

[37] N. Sharma, M. Parhizkar, W. Cong, S. Mateti, M. A. Kirland, M. Puri, A. Sutti, Metal ion type significantly affects the morphology but not the activity of lipase-metal-phosphate nanoflowers, RSC Adv, 7(2017) 25437-25443.

[38] C. Altinkaynak, S. Tavlasoglu, R. Kalin, N. Sadeghian, H. Ozdemir, I. Ocsoy, N. Özdemir, A hierarchical assembly of flower-like hybrid Turkish black radish peroxidase-Cu^{2+}nanobiocatalyst and its effective use in dye decolorization, Chemosphere. 182 (2017) 122–128.

[39] X. Fei, S. Chen, C. Huang, D. Liu, Y. Zhang, Immobilization of bovine carbonic anhydrase on glycidoxypropyl-functionalized nanostructured mesoporous silicas for carbonation reaction, J. Mol. Catal. B Enzym. 116 (2015) 134–139.

[40] P. Taslimi, F. Turkan, A. Cetin, H. Burhan, M. Karaman, I. Bildirici, I. Gulçin, F. Şen, Pyrazole[3,4-d]pyridazine derivatives: Molecular docking and explore of acetylcholinesterase and carbonic anhydrase enzymes inhibitors as anticholinergics potentials. Bioorg Chem. 2019, 92, 103213.

[41] C. Caglayan, P. Taslimi, C. Turk, F. M. Kandemir, Y. Demir, I. Gulçin, Purification and characterization of the carbonic anhydrase enzyme from horse mackerel (*Trachurus trachurus*) muscle and the impact of some metal ions and pesticides on enzyme activity. Comp Biochem Phys C. 2019, 226, 108605.

[42] S. Burmaoglu, A. O. Yilmaz, M. F. Polat, R. Kaya, I. Gulçin, O. Algul, Synthesis of novel tris-chalcones and determination of their inhibition profiles against some metabolic enzymes. Arch Phys Biochem. 2019, 43, e12908.

[43] S. Bayindir, C. Caglayan, M. Karaman, I. Gulcin, The green synthesis and molecular docking of novel N-substituted rhodanines as effective inhibitors for carbonic anhydrase and acetylcholinesterase enzymes. Bioorg Chem. 2019, 90, 103096.

[44] M. Topal, I. Gulcin, Rosmarinic acid: a potent carbonic anhydrase isoenzymes inhibitor. Turk J Chem. 2014, 38, 894-902.

[45] B. Arabaci, I. Gulcin, S. Alwasel, Capsaicin: A potent inhibitor of carbonic anhydrase isoenzymes. Molecules, 2014, 19, 10103-10114.

[46] X. L. Wang, J. F. Shi, Z. Li, S. H. Zhang, H. Wu, Z. Y. Jiang, C. Yang, C. Y. Tian, Facile one-pot preparation of chitosan/calcium pyrophosphate hybrid microflowers, ACS Appl. Mater. Interfaces 6 (2014) 14522−14532.

[47] P. Deshpande, A. Dapkekar, M. D. Oak, K. M. Paknikar, J. M. Rajwade, Zinc complexed chitosan/TPP nanoparticles: A promising micronutrient nanocarrier suited for foliar application, Carbohydr. Polym. 165 (2017) 394−401.

[48] L. Fan, H. Yang, J. Yang, M. Peng, J. Hu, Preparation and characterization of chitosan/gelatin/PVA hydrogel for wound dressings, Carbohydr. Polym. 146 (2016) 427−434.

[49] C. Garcia-Galan, A. Berenguer-Murcia, R. Fernandez-Lafuente, R. C. Rodrigues, Potential of different enzyme immobilization strategies to improve enzyme performance. Adv Synth Catal. 353(2011)2885-2904.

[50] M. H. Fu, J. F. Xing, Z. Q. Ge, Preparation of laccase-loaded magnetic nanoflowers and their recycling for efficient degradation of bisphenol A, Sci Total Environ. 651 (2019) 2857-2865.

[51] M. Y. Luo, M. F. Li, S. Jiang, H. Shao, J. Razal, D. Wang, Supported growth of inorganic-organic nanoflowers on 3D hierarchically porous nanofibrous membrane for enhanced enzymatic water treatment, J. Hazard Mater. 381 (2020) 120947.

[52] T. W. Tan, F. Wang, H. Zhang, Preparation of PVA/chitosan lipase membrane reactor and its application in synthesis of monoglyceride, J. Mol. Catal. B-Enzym. 18(2002) 325-331.

[53] M. Bilal, H. M. N. Iqbal, Naturally-derived biopolymers: Potential platforms for enzyme immobilization, Inter J. Biol. Macromol. 130(2019) 462-482.

[54] J. D. Cui, B. T. Sun, T. Lin, Y. X. Feng, S. R. Jia, Enzyme shielding by mesoporous organosilica shell on Fe3O4@silica yolk-shell nanospheres, Inter. J. Biol. Macromol. 117 (2018) 673-682.

[55] J. D. Cui, Y. X. Feng, S. R. Jia, Silica encapsulated catalase@metal-organic framework composite: A highly stable and recyclable biocatalyst, Chem Eng J. 351 (2018) 506-514.

[56] Y. Liu, Y. M. Zhang, X. J. Li, Q. P. Yuan, H. Liang, Self-repairing metal–organic hybrid complexes for reinforcing immobilized chloroperoxidase reusability, Chem. Commun. 53(2017) 3216.

Table 1 Mechanical properties

Tensile strength (Mpa)	Tensile stain at break εB (%)	Tensile yield stress σy (MPa)
0.984 ± 0.036	6.675 ± 0.399	0.570 ± 0.039

Figure legend

Figure 1 Schematic illustration of the preparation process for PVA/CS@CANF composite membrane.

Figure 2 SEM images of (a) CA/$Cu_3(PO_4)_2$ hybrid nanoflowers, (b) CA/$Zn_3(PO_4)_2$ hybrid nanoflowers, (c) Bimetal based inorganic-carbonic anhydrase hybrid nanoflowers, (d) blank PVA/CS hydrogel membrane, (e) PVA/CS@CANF composite membrane, (f) high resolution image of PVA/CS@CANF.

Figure 3 FTIR spectra of CA, $Cu_3(PO_4)_2$, PVA/CS hydrogels, CANF, and PVA/CS@CANF.

Figure 4 CLSM of (a) CANF and (b) PVA/CS@CANF.

Figure 5 The elemental analysis of PVA/CS@CANF.

Figure 6 Comparison of activity recovery of CA/$Cu_3(PO_4)_2$, CA/$Zn_3(PO_4)_2$ and CANF(a); Effect of the ratio of PVA and CS on the activity of PVA/CS@CANF(b); Effect of temperature (c) and pH (b) on the activity of free CA, CANF and PVA/CS@CANF.

Figure 7 Stability of free CA, CANF, and PVA/CS@CANF. (a) thermostability; (b) pH stability; (c) storage ability; (d) reusability.

Figure 8 Comparison of conversion of carbon dioxide into $CaCO_3$. SEM images of calcium carbonate crystals obtained in the presence of (a) free CA, (b) CANF, and (c) PVA/CS@CANF.

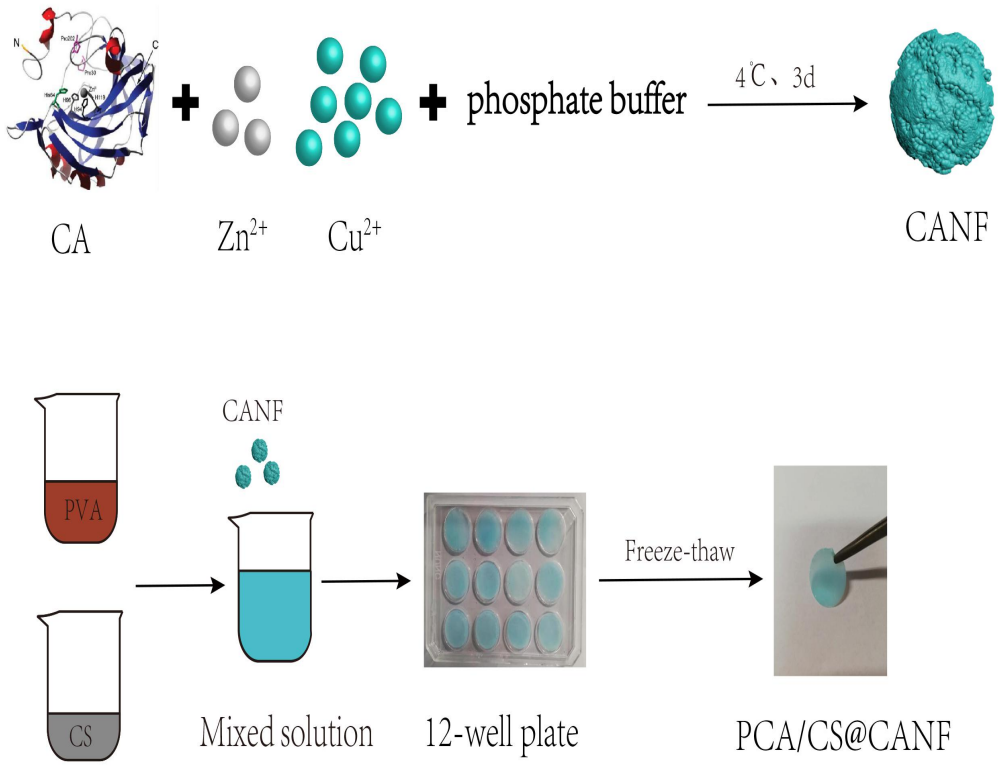
phosphate buffer
4℃、3d
CA
Zn2+
Cu2+
CANF
CANF
PVA
CS
Mixed solution
12-well plate
Freeze-thaw
PCA/CS@CANF

Fig. 1

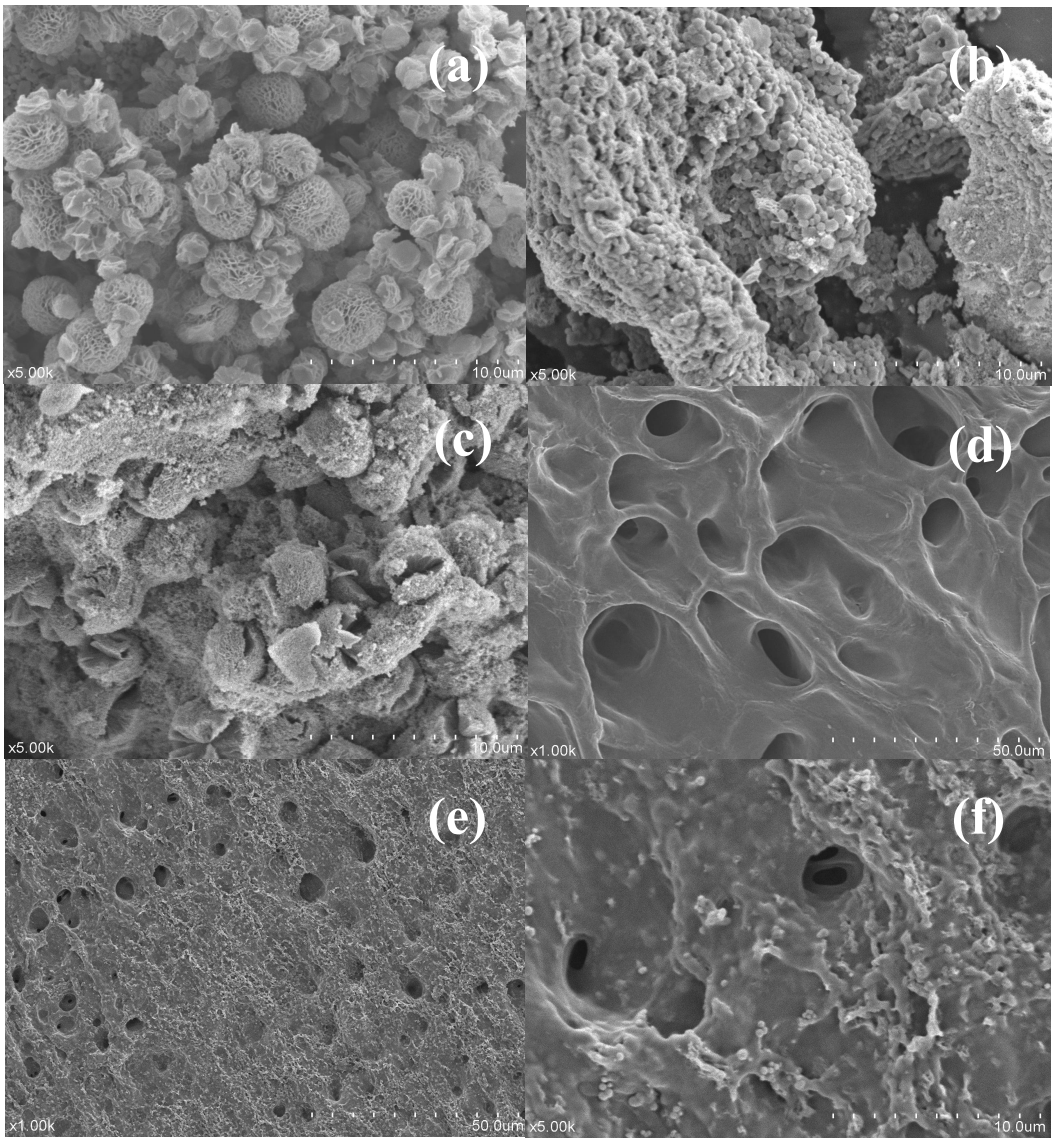
(a)
x5.00k
10.0um
(b)
x5.00k
10.0um
(c)
x5.00k
10.0um
(d)
x1.00k
50.0um
(e)
x1.00k
50.0um
(f)
x5.00k
10.0um

Fig. 2

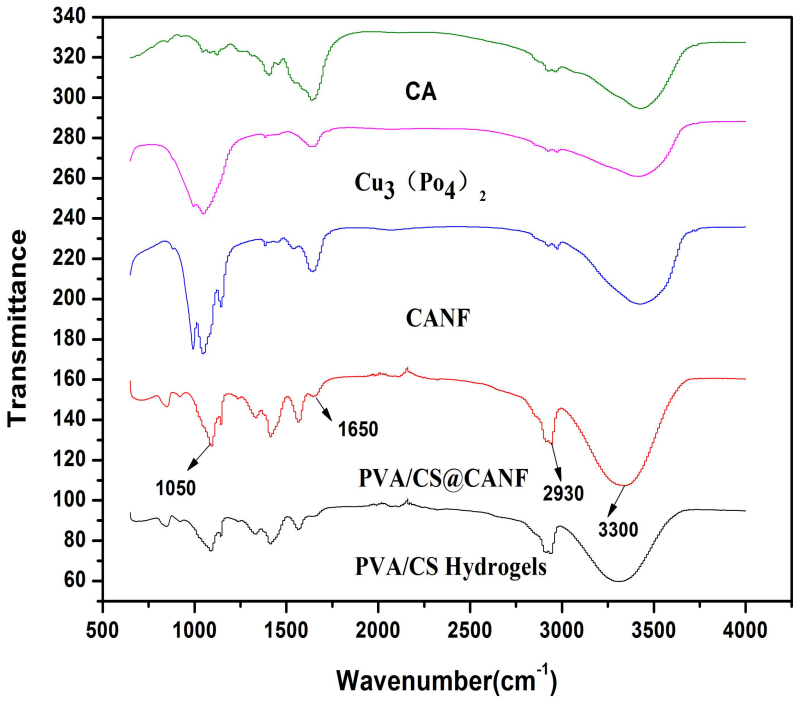
Transmittance
Wavenumber(cm-1)
CA
Cu3（Po4）2
CANF
PVA/CS@CANF
PVA/CS Hydrogels
1650
1050
2930
3300

Fig. 3

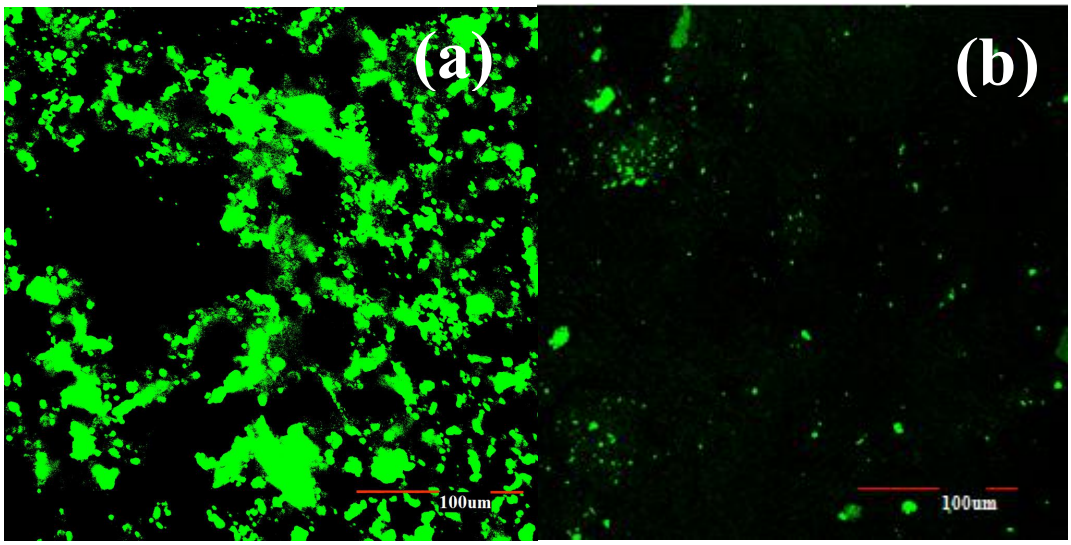

Fig. 4

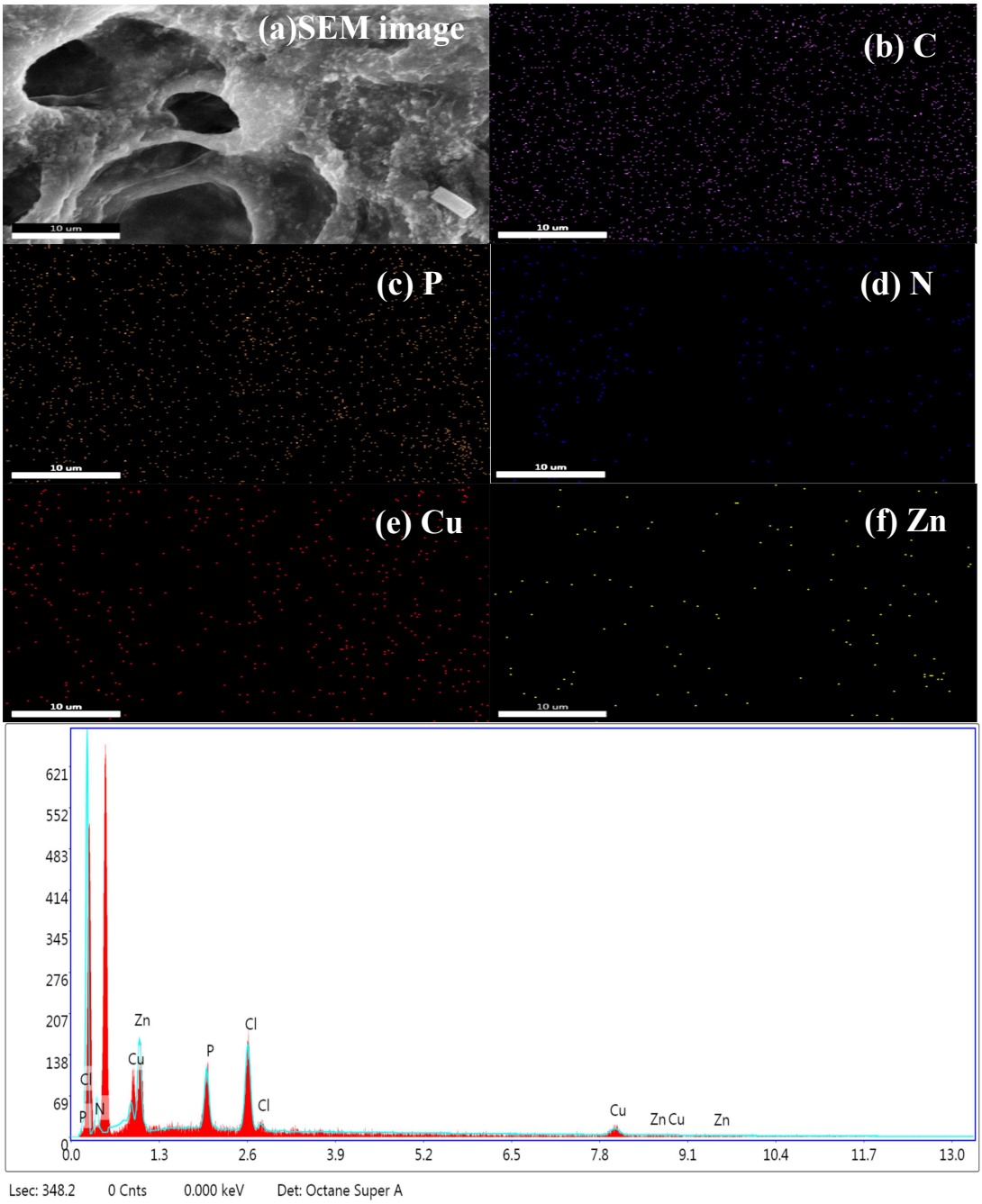
(a)SEM image
(b) C
(c) P
(d) N
(e) Cu
(f) Zn
10 um
621
552
483
414
345
276
207
138
69
0
Zn
Cu
P
Cl
Cl
Cl
P
N
Cu
Zn Cu
Zn
0.0
1.3
2.6
3.9
5.2
6.5
7.8
9.1
10.4
11.7
13.0
Lsec: 348.2
0 Cnts
0.000 keV
Det: Octane Super A

Fig. 5

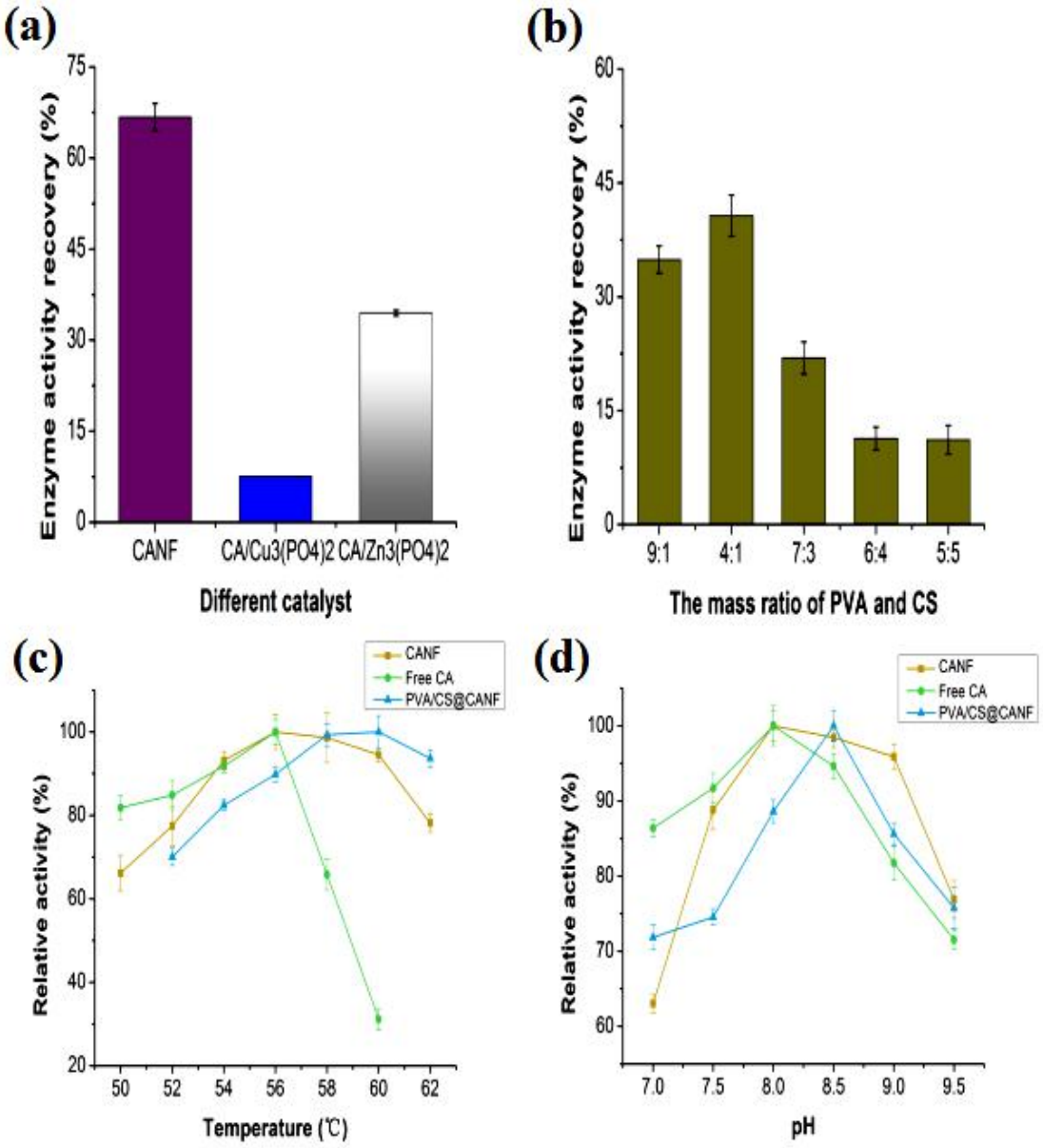
(a)
Enzyme activity recovery (%)
75
60
45
30
15
0
CANF
CA/Cu3(PO4)2
CA/Zn3(PO4)2
Different catalyst
(b)
Enzyme activity recovery (%)
60
45
30
15
0
9:1
4:1
7:3
6:4
5:5
The mass ratio of PVA and CS
(c)
CANF
Free CA
PVA/CS@CANF
Relative activity (%)
100
80
60
40
20
50
52
54
56
58
60
62
Temperature (℃)
(d)
CANF
Free CA
PVA/CS@CANF
Relative activity (%)
100
90
80
70
60
7.0
7.5
8.0
8.5
9.0
9.5
pH

Fig. 6

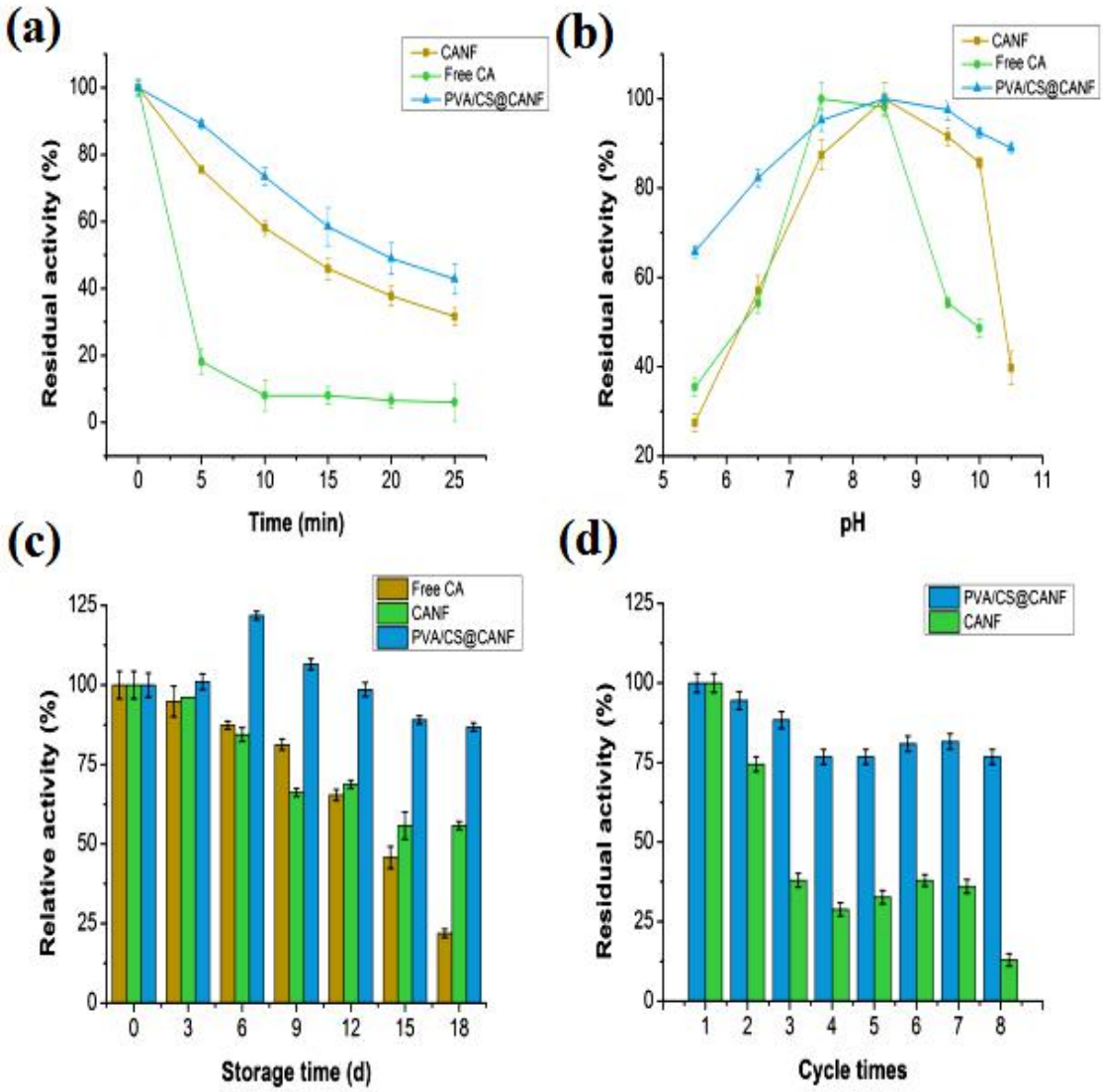
(a)
CANF
Free CA
PVA/CS@CANF
Residual activity (%)
Time (min)
(b)
CANF
Free CA
PVA/CS@CANF
Residual activity (%)
pH
(c)
Free CA
CANF
PVA/CS@CANF
Relative activity (%)
Storage time (d)
(d)
PVA/CS@CANF
CANF
Residual activity (%)
Cycle times

Fig. 7

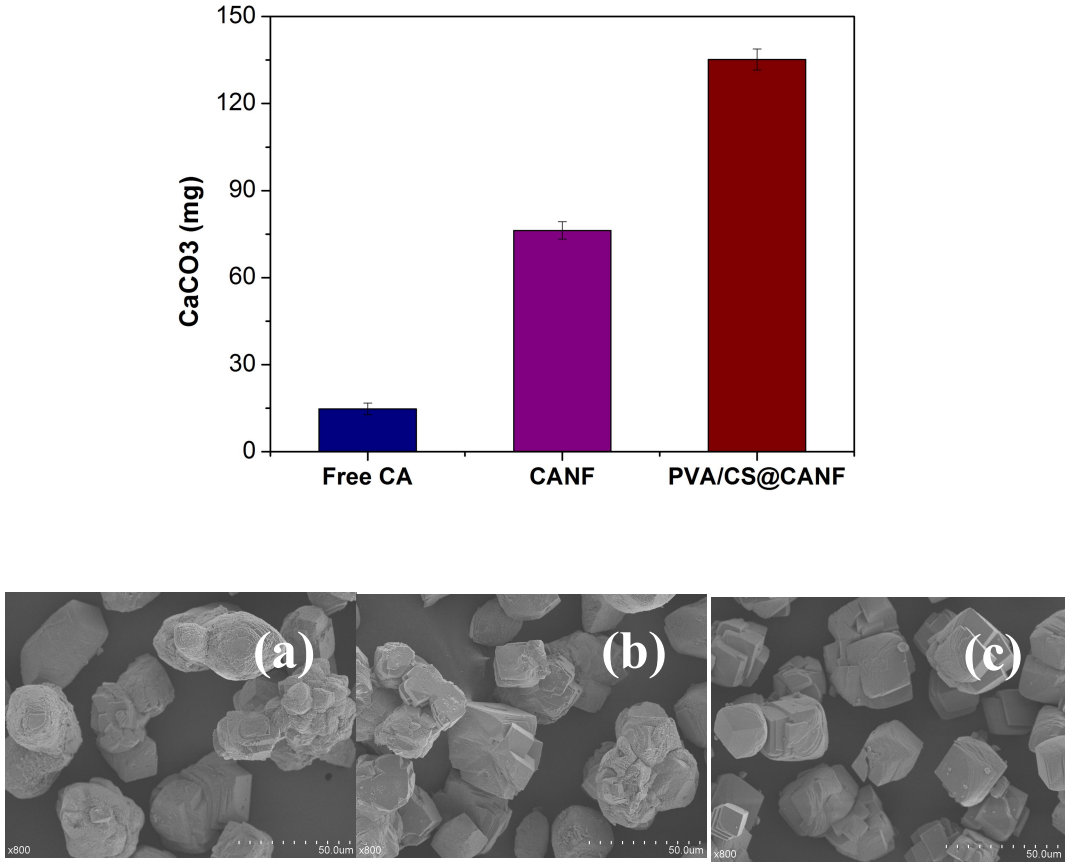

Fig. 8

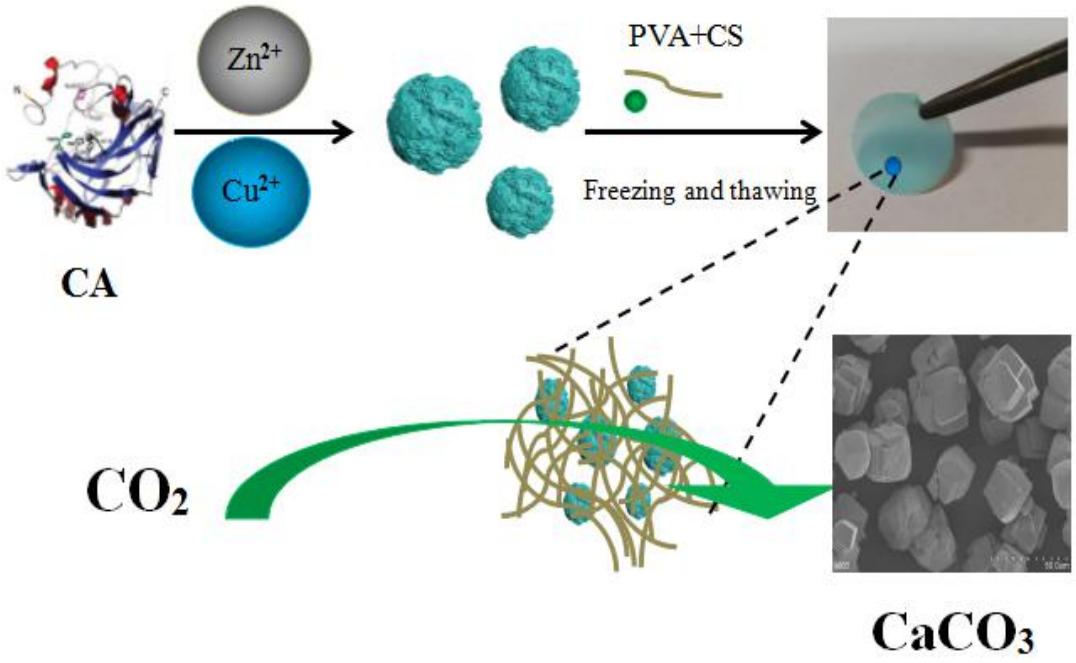

Graphical abstract